

# Long-Chain Acylcarnitines Regulate the hERG Channel

Fabio Ferro<sup>1,9</sup>, Aude Ouillé<sup>2,9</sup>, Truong-An Tran<sup>1</sup>, Pierre Fontanaud<sup>3</sup>, Patrick Bois<sup>4</sup>, Dominique Babuty<sup>5</sup>, François Labarthe<sup>1</sup>, Jean-Yves Le Guennec<sup>2</sup>

**1** INSERM U921, Université François-Rabelais, Tours, France, **2** INSERM U1046, Université Montpellier-1, Université Montpellier-2, Montpellier, France, **3** IGF-CNRS INSERM 661, Université Montpellier-1, Université Montpellier-2, Montpellier, France, **4** IPBC, UMR 6187, CNRS, Université de Poitiers, Poitiers, France, **5** CHRU Tours, Hôpital Trousseau, Service de cardiologie B, Tours, France

## Abstract

**Background and purpose:** In some pathological conditions carnitine concentration is high while in others it is low. In both cases, cardiac arrhythmias can occur and lead to sudden cardiac death. It has been proposed that in ischaemia, acylcarnitine (acyl-CAR), but not carnitine, is involved in arrhythmias through modulation of ionic currents. We studied the effects of acyl-CARs on hERG,  $K_{IR2.1}$  and  $K_{V7.1/minK}$  channels (channels responsible for  $I_{KR}$ ,  $I_{K1}$  and  $I_{KS}$  respectively).

**Experimental approach:** HEK293 cells stably expressing hERG,  $K_{IR2.1}$  or  $K_{V7.1/minK}$  were studied using the patch clamp technique. Free carnitine (CAR) and acyl-CAR derivatives from medium- (C8 and C10) and long-chain (C16 and C18:1) fatty acids were applied intra- and extracellularly at different concentrations. For studies on hERG, C16 and C18:1 free fatty acid were also used.

**Key results:** Extracellular long-chain (LCAC), but not medium-chain, acyl-CAR, induced an increase of  $I_{hERG}$  amplitude associated with a dose-dependent speeding of deactivation kinetics. They had no effect on  $K_{IR2.1}$  or  $K_{V7.1/minK}$  currents. Computer simulations of these effects were consistent with changes in action potential profile.

**Conclusions and applications:** Extracellular LCAC tonically regulates  $I_{hERG}$  amplitude and kinetics under physiological conditions. This modulation may contribute to the changes in action potential duration that precede cardiac arrhythmias in ischaemia, diabetes and primary systemic carnitine deficiency.

**Citation:** Ferro F, Ouillé A, Tran T-A, Fontanaud P, Bois P, et al. (2012) Long-Chain Acylcarnitines Regulate the hERG Channel. PLoS ONE 7(7): e41686. doi:10.1371/journal.pone.0041686

**Editor:** Alexander G. Obukhov, Indiana University School of Medicine, United States of America

**Received:** January 30, 2012; **Accepted:** June 25, 2012; **Published:** July 25, 2012

**Copyright:** © 2012 Ferro et al. This is an open-access article distributed under the terms of the Creative Commons Attribution License, which permits unrestricted use, distribution, and reproduction in any medium, provided the original author and source are credited.

**Funding:** This work was financially supported by Boston Scientific and the conseil Régional du Centre. The funders had no role in study design, data collection and analysis, decision to publish, or preparation of the manuscript.

**Competing Interests:** The authors have read the Journal's policy and have the following conflicts: They have received funding from Boston Scientific. There are no patents, products in development or marketed products to declare. This does not alter the authors' adherence to all the PLoS ONE policies on sharing data and materials.

\* E-mail: aude.ouille@inserm.fr

<sup>9</sup> These authors contributed equally to the work.

## Introduction

Fatty acids are the primary substrate used by the heart to generate ATP [1]. The initial steps involved in ATP production via  $\beta$ -oxidation include the formation of essential intermediates that facilitate the transport of fatty acids into the mitochondrial matrix where the  $\beta$ -oxidation enzymes are located. More specifically, after their entry into the cell, fatty acids are activated in the cytosol via the formation of acyl-CoA derivatives, which are either incorporated into intracellular lipid pools or enter mitochondria for  $\beta$ -oxidation. Carnitine (CAR) is the essential co-factor needed for mitochondrial fatty acid oxidation. It operates by shuttling long-chain fatty acids as acylcarnitine esters (acyl-CAR) from the cytoplasm across the inner mitochondrial membrane into the mitochondrial matrix. After their entry into the mitochondria, long-chain acyl-CAR (LCAC) are converted back to long-chain acyl-CoA esters, which are then  $\beta$ -oxidized into acyl-CoA of progressively shorter chain lengths (i.e. long-, medium-, short-chain acyl-CoA, and ultimately acetyl-CoA). Free carnitine is then recycled [2]. In contrast to acyl-CoA, acyl-CARs diffuse easily through the mitochondrial and plasma membranes.

Thus their blood concentration reflects the fluxes of various mitochondrial  $\beta$ -oxidation steps. This process is also suspected to be protective against the accumulation of potentially toxic acyl-CoA derivatives in mitochondria and to preserve free CoA availability for energy metabolism [3].

In normal myocardium, the concentration of acyl-CARs is low, around 2–3  $\mu$ M, because the transformation of cytosolic acyl-CoA into acyl-CAR is tightly coupled to myocardial energy demand [4–6]. Acyl-CARs are synthesized in the cell and they can easily diffuse through the cell membrane and reach the cytosol.

Free fatty acid and acyl-CAR concentrations can increase in some pathological conditions such as myocardial ischaemia [7], diabetes [8], [9] and genetic fatty acid disorders [10]. The arrhythmias observed in these conditions could be due to a perturbation of cardiomyocyte repolarisation by carnitine or its derivatives.

In pathological conditions such as primary systemic carnitine deficiency or ischaemia, acyl-CARs can either decrease to immeasurably low levels [2] or increase to 30  $\mu$ M [11] respectively. It has been found that long chain acyl-CARs

modulate the activity of certain calcium and sodium channels at a concentration of 5–10  $\mu\text{M}$  [12–13]. However, the effects of acyl-CARs on outward currents participating in repolarization (hERG, Kv7.1/minK and KIR2.1 channels) have not been studied. Changes in the activity of these potassium channels are known to be associated with ventricular fibrillation and sudden death [14–15]. These arrhythmias could be either due to  $\text{K}^+$  channel blockade, by drugs or loss-of-function by mutations (long QT syndrome), or due to their activation by hyperkalemia, acidosis, digitalis toxicity, hyperthermia [16], or gain-of-function mutations [17].

The purpose of this study was to evaluate the effects of different concentrations of medium- and long-chain acyl-CARs on these repolarising potassium channels. A physiological concentration of 3  $\mu\text{M}$  acyl-CAR [5–6], [18], was compared to very low and high acyl-CAR concentrations, applied either intra- or extracellularly.

## Methods

### Cell Culture

HEK293 cells expressing Kv11.1 (hERG channel) were a kind gift from Drs Zhou and January (Madison, USA) [19]. HEK293(LGC Promochem, France) expressing Kv7.1 associated with minK subunit (*KCNE1* gene) and KIR2.1 channel (*KCNJ2* gene,  $\text{I}_{\text{K1}}$ ) were made inhouse. Cells were seeded in 25  $\text{cm}^2$  cell-culture flasks at 37°C and 10%  $\text{CO}_2$  and grown in DMEM Dulbecco's modified Eagle's medium supplemented with 10% (v/v) Fetal Bovine Serum (Cambrex Bio Science Verviers, Belgium). HEK-hERG medium was supplemented with 0.4 mg/ml geneticin (Gibco, Invitrogen Corporation, UK). Culture medium was changed every 2–3 days. Within 7 days, cells were at approximately 80% of confluence. The cells were then harvested using a Dulbecco Phosphate Buffered Saline without calcium and magnesium (DPBS, Cambrex Bio Science Verviers, Belgium) and trypsin (Lonza, Belgium) and seeded in a new culture flask (60000 cells/flask) for following week. Cells were also seeded in 35 mm Petri dishes to obtain a confluence of about 50% on the day of experimentation. Cells were mycoplasma negative.

### Whole-cell patch-clamp Recording

Cells were placed on the stage of an inverted microscope (Nikon TE2000-U, Japan). Patch-clamp techniques have been described in detail elsewhere [20]. Currents were recorded by whole-cell voltage clamp with a Biologic RK-400 amplifier (Biologic, Grenoble, France) and an Axopatch 200 B (Axon Instrument, La Jolla, USA). Currents were filtered at 3 kHz (Axopatch) or 2 kHz (Biologic) and sampled at 5 kHz. Borosilicate glass electrodes (GC150F-15, Harvard Apparatus, UK) with tip resistances of 3.5–5  $\text{M}\Omega$  when filled with the internal solution for  $\text{I}_{\text{KR}}$  and  $\text{I}_{\text{K1}}$  channel. This solution contained (in mM): KCl 130,  $\text{MgCl}_2$  1, Mg-ATP 5, EGTA 5, HEPES 10, adjusted to pH 7.2 with KOH. The internal solution for studying  $\text{I}_{\text{KS}}$  was (in mM): KCl 130,  $\text{MgCl}_2$  1, NaCl 10,  $\text{CaCl}_2$  1, HEPES 5, adjusted to pH 7.2 with KOH. The external physiological saline solution (PSS) contained (in mM): NaCl 137, KCl 4,  $\text{MgCl}_2$  1,  $\text{CaCl}_2$  1.8, D-Glucose 10, and HEPES 10, adjusted to pH 7.4 with NaOH. For HEK- $\text{I}_{\text{KS}}$  experiments we used the perforated-patch configuration which was obtained with 0.250 mg/ml nystatin (Sigma-Aldrich, St Quentin Fallavier, France). Experiments were conducted at  $23 \pm 1^\circ\text{C}$ . Junction potentials were zeroed before formation of the membrane-pipette seal. Series resistance and capacitance were compensated. Current amplitudes were normalized to cell capacitance and expressed as current density (pA/pF). Cell capacitance ranged between 10 to 20 pF. The cell under study

was positioned at the tip of a conical microcapillary that received the outlet of six microcapillaries connected to 10 ml syringes. Superfusion was gravity-driven at 0.4 ml/min.

**$\text{I}_{\text{HERG}}$  protocols.** Cells were held at a membrane potential of  $-70$  mV. After control data were obtained, the superfusion was switched to the chosen acyl-CAR-containing solution, fatty-acid-containing-solution, or E4031-containing solution. Currents were elicited by 5 s test pulses to  $-10$  mV applied every 18 s until steady-state was obtained. Steady-state current-voltage relationships (IV) were obtained by stepping the membrane voltage for 5 s to voltages between  $-80$  and  $+50$  mV by 10 mV increments. Deactivating tail currents were recorded at  $-55$  mV. The activation curves were obtained from the tail current amplitude measured at its peak value. The availability curves were obtained from the maximum current amplitude measured at a test pulse to  $+40$  mV, applied after a two-pulse protocol that consisted of a 1 s depolarizing pulse to  $+40$  mV followed by a second 25 ms pulse to different membrane potentials between  $-120$  and  $+10$  mV. At the end of each experiment, the cell under study was perfused with E-4031 30 nM (a hERG blocker) (Alomone Labs, Jerusalem, Israel).

**$\text{I}_{\text{K1}}$  protocol.** Cells were held at a membrane potential of  $-90$  mV. A voltage ramp protocol of 1 s duration, from  $-120$  to  $+40$  mV was applied each 11 s. We measured the peak inward current, in the presence or absence of acyl-CAR. At the end of each experiment, the cell under study was perfused with  $\text{BaCl}_2$  150  $\mu\text{M}$  (an  $\text{I}_{\text{K1}}$  blocker) (Sigma-Aldrich, St Quentin Fallavier, France).

**$\text{I}_{\text{KS}}$  protocols.** Cells were held at a membrane potential of  $-70$  mV. Steady-state current-voltage relationships (IV) were obtained by stepping the membrane voltage for 3.5 s between  $-60$  and  $+40$  mV in 10 mV increments. Deactivating tail currents were recorded at  $-30$  mV. The activation curves were obtained from the peak tail current amplitude. At the end of each experiment, the cell under study was perfused with Chromanol 293 B15  $\mu\text{M}$  (an  $\text{I}_{\text{KS}}$  blocker) (Sigma-Aldrich, St Quentin Fallavier, France).

Command potentials, data acquisition and analysis were generated using Clampex 8.2 (Axon Instrument, Foster City, CA, USA).

Deactivating currents were best described by two exponentials using the following equation:

**Table 1.** Effect of application of intra- or extracellular acyl-CARs on  $\text{I}_{\text{HERG}}$  deactivation time constants. The hERG current was fitted to a two exponential function (see Methods for details).

Treatment		Tau 1 Mean $\pm$ SEM	Tau 2 Mean $\pm$ SEM	n
Control		1663 $\pm$ 118.5	314.4 $\pm$ 26.5	12
Intracellular	3 $\mu\text{M}$ C8-CAR	1378.6 $\pm$ 75.1	263.3 $\pm$ 12.1	8
	3 $\mu\text{M}$ C10-CAR	1467.6 $\pm$ 64.5	306.6 $\pm$ 10.6	7
	3 $\mu\text{M}$ C16-CAR	1658.4 $\pm$ 105.8	323.5 $\pm$ 15.8	12
	3 $\mu\text{M}$ C18-CAR	1440.4 $\pm$ 120.6	288.8 $\pm$ 26.6	9
Extracellular	3 $\mu\text{M}$ C8-CAR	1488.6 $\pm$ 87.1	275.8 $\pm$ 11.8	8
	3 $\mu\text{M}$ C10-CAR	1667.9 $\pm$ 101.1	301.5 $\pm$ 17.8	7
	3 $\mu\text{M}$ C16-CAR	1077.1 $\pm$ 139.7**	222.2* $\pm$ 21.3	7
	3 $\mu\text{M}$ C18-CAR	1059.4 $\pm$ 88.7**	212.6* $\pm$ 18.9	8

The values of tau1 and tau2 are given in ms. Values were obtained when the membrane potential returned to  $-55$  mV after stepping to  $-10$  mV for 5s. \* $p < 0.05$ , \*\*  $p < 0.01$ .

doi:10.1371/journal.pone.0041686.t001

$$I = A_0 + A_1 \cdot \exp(-t/\tau_1) + A_2 \cdot \exp(-t/\tau_2).$$

where  $\tau_1$  and  $\tau_2$  are the time constants,  $A_1$  and  $A_2$  are the amplitude of the 1<sup>st</sup> and 2<sup>nd</sup> component of the exponential respectively and  $A_0$  the amplitude of the remaining current.

Half-maximal voltages ( $V_{1/2}$ ) of activation and availability were determined by fitting data with a Boltzmann equation:

$$I/I_{max} = 1 / \{1 + \exp[-(E - V_{1/2})/s]\}.$$

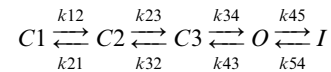
where  $I/I_{max}$  represents the normalized current,  $V_{1/2}$  the half-maximal voltages of activation or availability and  $s$  the slope factor. These analyses were performed using Origin 7 (Microcal Software, Northampton, MA, USA).

Acyl-CARs(except oleylcarnitine) were purchased from Drten Brink (Amsterdam, Netherland). Oleylcarnitine and chemicals were purchased from Sigma-Aldrich (St Quentin Fallavier, France). Two medium-chain acyl-CAR derivatives were used: octanoylcarnitine (C8-CAR) and decanoylcarnitine (C10-CAR) and two long-chain palmitoylcarnitine (C16-CAR) and oleylcarnitine (C18-CAR).

To simplify the terminology, we indicate the number of carbon atoms in the aliphatic chain. We used C18:1-CAR rather than C18:0-CAR because the C18:1 carnitine derivative is more abundant in the myocardium than C18:0, in both physiological and pathophysiological conditions [18]. A stock solution of 30 mM Acyl-CARs, dissolved in water, was diluted to experimental concentrations between 1 and 30  $\mu$ M.

**Mathematical Modelling**

The model used in this study is the human endocardial ventricular cell model described by Ten Tusscher & Panvilov [21] in which we replaced the Hodgkin-Huxley equation for  $I_{KR}$  by a Markov equation. Following Fink *et al.* [22] we chose to describe  $I_{KR}$  using the following Markov chain which had 3 closed states, one open state and one inactivated state:



The simplex method was used to fit the experimental data using JSim software.

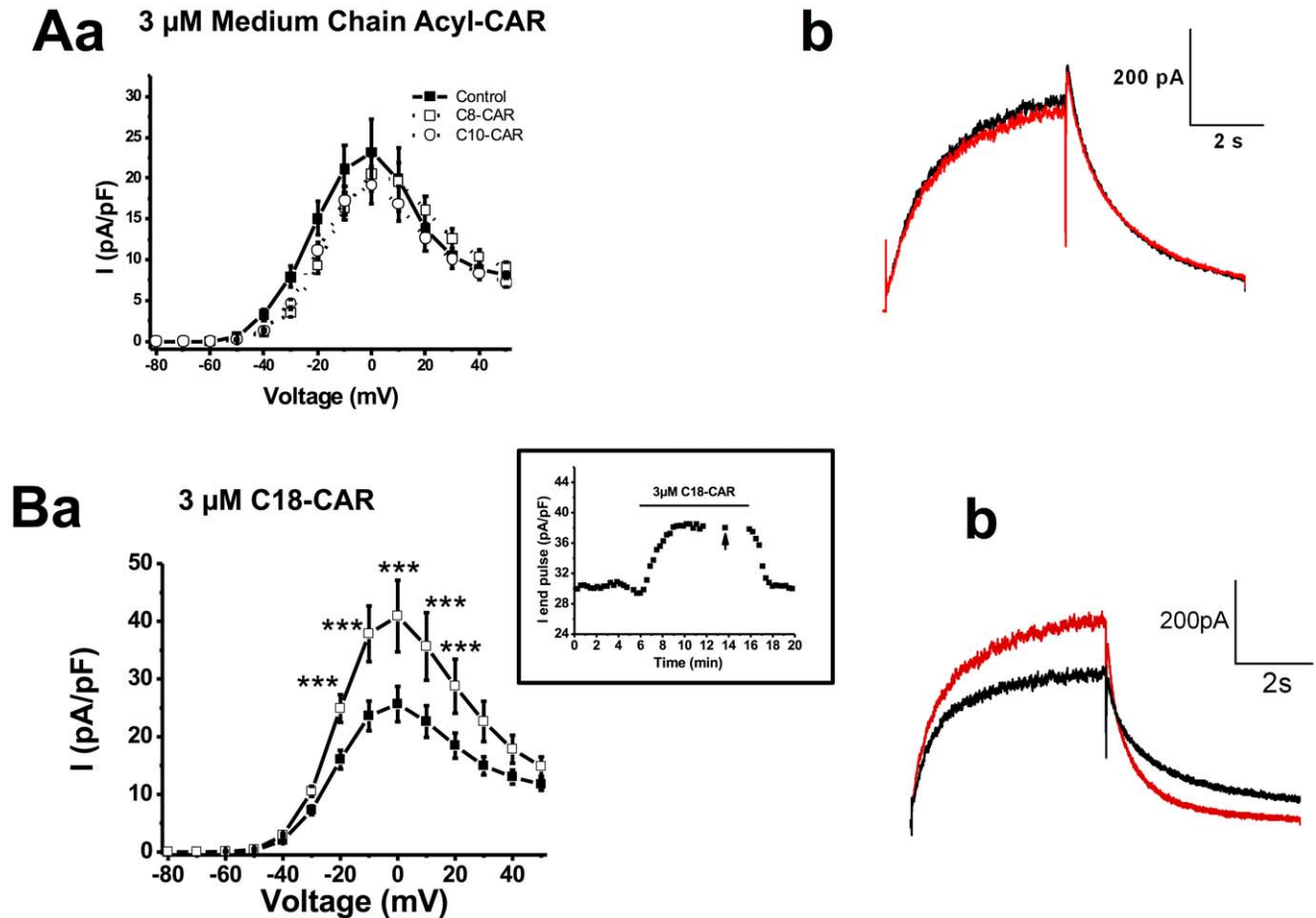


**Figure 1. Effect of extracellular acyl-CARs on  $I_{hERG}$ .**  $I_{hERG}$ - $V$  relationships, in all graphs, the filled squares represent the current in the absence of acyl-CAR in the pipette (control,  $n = 12$  cells). **Aa**, effect of 3  $\mu$ M C8-CAR (empty circles,  $n = 8$  cells) or 3  $\mu$ M C10-acyl-CAR (filled circles,  $n = 7$  cells); **Ab**, typical example of C8-CAR (red) compared with PSS (black). **Ba**, effect of 3  $\mu$ M C18-CAR (filled circles,  $n = 9$  cells) on  $I_{hERG}$ - $V$  relationship. The inset shows the effect of 3  $\mu$ M C18-CAR on end-pulse hERG current elicited by a depolarisation to  $-10$  mV from a holding voltage of  $-70$  mV, obtained on a representative cell (the arrows indicate the current obtained at  $-10$  mV during an IV protocol, see Methods), \*\*\*,  $p < 0.001$ . \*\*,  $p < 0.01$ . **Bb**, typical example of C18-CAR (red) compared with PSS (black). doi:10.1371/journal.pone.0041686.g001

The reaction constants were:  
 $k_{12} = 0.01507341 \cdot \exp(0.001459408 \cdot V)$  in PSS and  $k_{12} = 0.02007341 \cdot \exp(0.07865593 \cdot V)$  in the presence of C16-CAR.  
 $k_{21} = 0.05364064 \cdot \exp(-0.19822938 \cdot V)$  in PSS and  $k_{21} = 0.2364064 \cdot \exp(-0.00011822938 \cdot V)$  in the presence of C16-CAR.  
 $k_{23} = 0.08927204$  in PSS and  $k_{23} = 0.02927204$  in the presence of C16-CAR.  
 $k_{32} = 15686841$  in PSS and  $k_{32} = 0.01686841$  in the presence of C16-CAR.  
 $k_{34} = 0.01066403 \cdot \exp(0.00131023 \cdot V)$  in PSS and  $k_{34} = 0.15066403 \cdot \exp(0.0231023 \cdot V)$  in the presence of C16-CAR.

$k_{43} = 0.0005743 \cdot \exp(-0.0006156 \cdot V)$  in PSS and  $k_{43} = 0.00037433 \cdot \exp(-0.04078603 \cdot V)$  in the presence of C16-CAR.

$k_{45} = 0.05042237 \cdot \exp(0.00854485 \cdot (V+18))$  in PSS and  $k_{45} = 0.16042237 \cdot \exp(0.01554485 \cdot (V+4.5))$  in the presence of C16-CAR.

$k_{54} = 0.01731608 \cdot \exp(-0.04090733 \cdot (V+18))$  in PSS and  $k_{54} = 0.03731608 \cdot \exp(-0.05090733 \cdot (V+4.5))$  in the presence of C16-CAR.

**Statistics**

Data are described as mean ± standard error of the mean (n = number of cells). Two-way repeated measures ANOVA followed

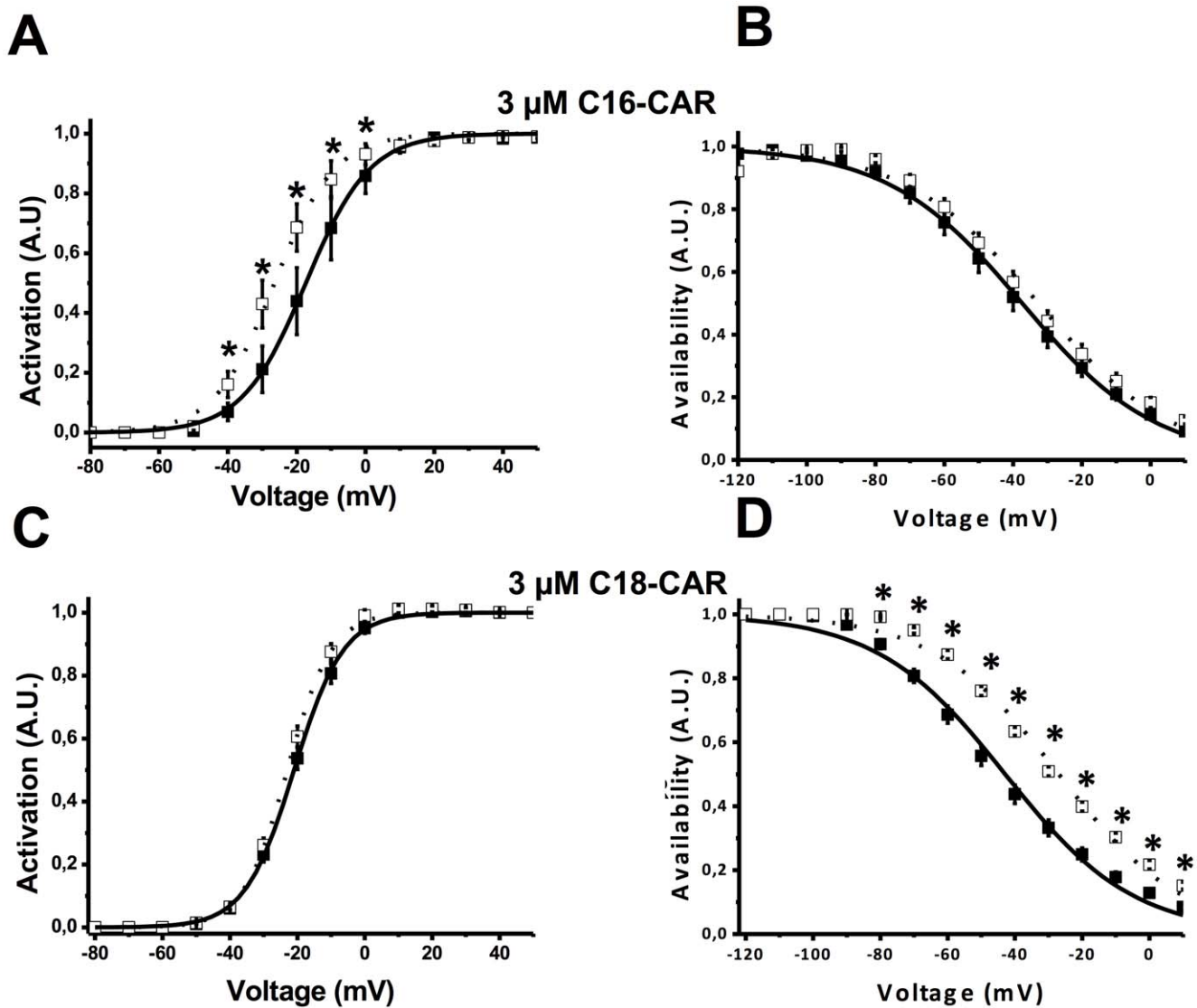


**Figure 2. Effect of extracellular long-chain acyl-CARs on the activation and availability of the hERG current.** **A**, effect of 3 μM C16-CAR on the activation curve. In the absence of C16-CAR (filled squares, n=6 cells), the  $V_{1/2}$  is  $-17.4 \pm 0.2$  mV while in the presence of 3 μM acyl-CAR (empty squares) the  $V_{1/2}$  is  $-26.5 \pm 0.5$  mV. **B**, effect of 3 μM C16-CAR on availability. In the absence of C16-CAR (empty squares, n=6 cells), the  $V_{1/2}$  is  $-35.4 \pm 1.4$  mV while in the presence of 3 μM acyl-CAR (filled squares) the  $V_{1/2}$  is  $-37.4 \pm 0.5$  mV. **C**, effect of 3 μM C18-CAR on activation. In the absence of C18-CAR (filled squares, n=7 cells), the  $V_{1/2}$  is  $-21.0 \pm 0.1$  mV while in the presence of 3 μM acyl-CAR (empty squares) the  $V_{1/2}$  is  $-23.0 \pm 0.2$  mV. **D**, effect of 3 μM C18-CAR on availability. In the absence of C18-CAR (filled squares, n=7 cells) the  $V_{1/2}$  is  $-42.9 \pm 1.0$  mV while in the presence of 3 μM acyl-CAR (empty squares) the  $V_{1/2}$  is  $-27.0 \pm 1.0$  mV. \* :  $p < 0.01$ . doi:10.1371/journal.pone.0041686.g002

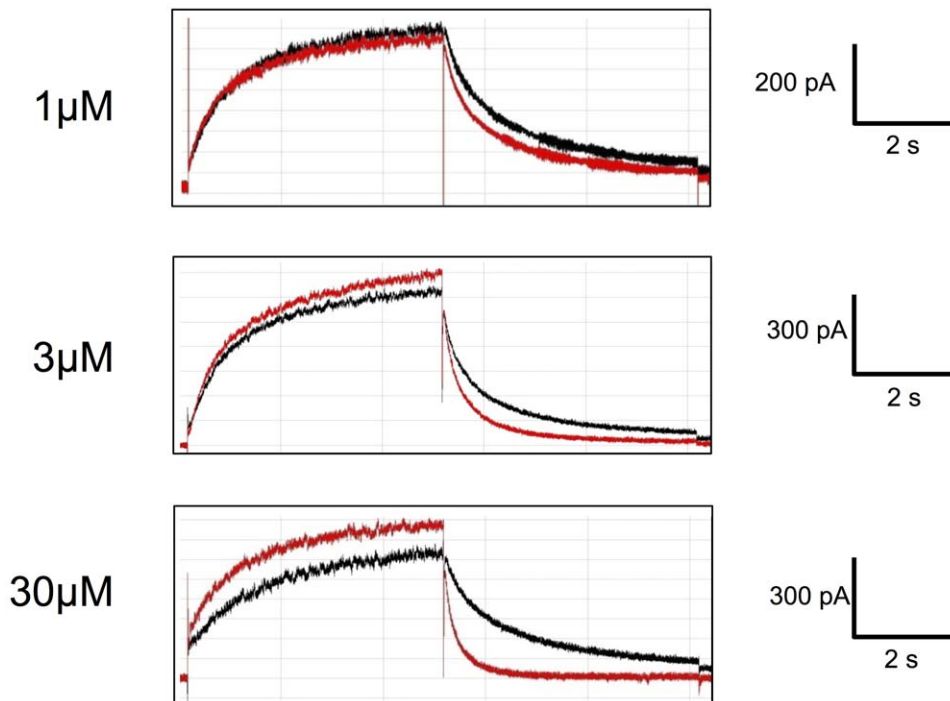


**Figure 3. Concentration-dependent acceleration of  $I_{hERG}$  inactivation induced by C18-CAR.** The records were obtained in 3 different cells. The current obtained in presence of C18-CAR is shown in red.  
doi:10.1371/journal.pone.0041686.g003

by a Student–Newmann–Keuls test were used to compare current densities. To compare the effects of acyl-CARs on the kinetics of deactivation, we performed unpaired (intracellular) and paired (extracellular) Student’s t-test. Differences were considered as statistically significant when  $p < 0.05$ .

**Results**

**Acylcarnitines have no Impact on  $I_{hERG}$  when Applied Intracellularly**

We compared  $I_{hERG}$  in the absence or presence of intracellular free carnitine, medium-chain acyl-CARs (e.g. C8-

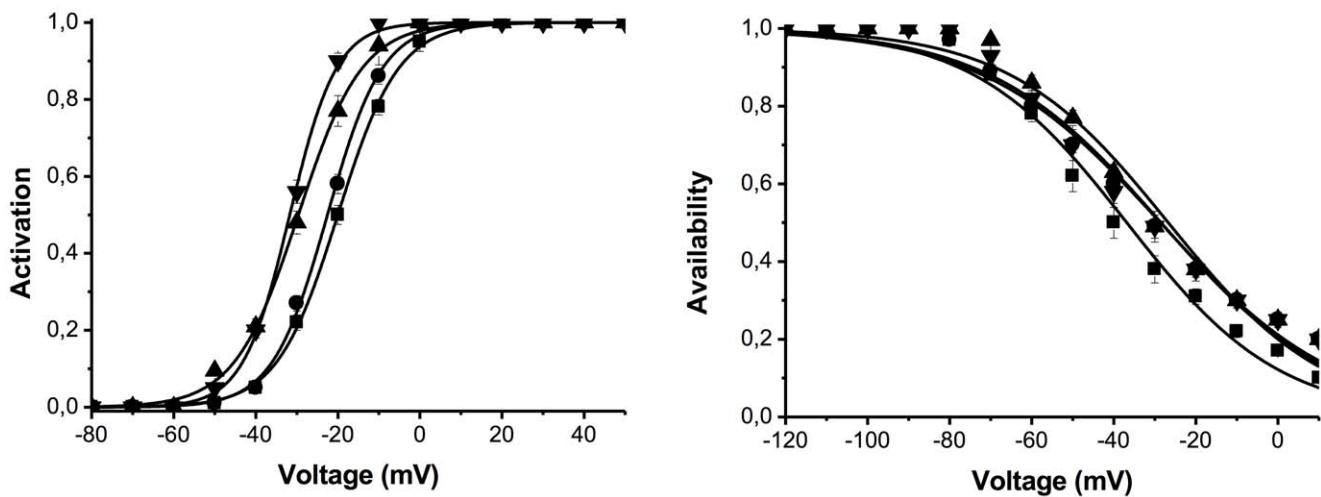


**Figure 4. Effect of extracellular C18-CAR on hERG activation and availability.** **A.** Activation curve in PSS (squares):  $V_{1/2} = -20.3 \pm 0.1$  mV ( $n = 10$ ); in the presence of  $1 \mu\text{M}$  C18-CAR (circles):  $-22.8 \pm 0.1$  mV ( $n = 8$ ); in the presence of  $3 \mu\text{M}$  C18-CAR (diamonds):  $-30.0 \pm 0.3$  mV ( $n = 8$ ) and in the presence of  $10 \mu\text{M}$  C18-CAR (triangles):  $-31.9 \pm 0.9$  mV ( $n = 4$ ). **B.** Availability curve in PSS (squares):  $V_{1/2} = -40.9 \pm 2.3$  mV ( $n = 8$ ); in the presence of  $1 \mu\text{M}$  C18-CAR (circles):  $V_{1/2} = -36.2 \pm 3.1$  mV ( $n = 8$ ); in the presence of  $3 \mu\text{M}$  C18-CAR (triangles):  $V_{1/2} = -34.8 \pm 1.4$  mV ( $n = 8$ ) and in the presence of  $10 \mu\text{M}$  C18-CAR (diamonds):  $V_{1/2} = -35.6 \pm 2.1$  mV.  
doi:10.1371/journal.pone.0041686.g004

**Table 2.** Effect of different concentrations of extracellular C18-CAR on  $I_{hERG}$  deactivation time constants.

Treatment	Tau1		Tau2	
	Mean $\pm$ SEM	n	Mean $\pm$ SEM	n
PSS	2331 $\pm$ 160	13	469 $\pm$ 37	13
C18-CAR 1 $\mu$ M	2289 $\pm$ 154	8	431 $\pm$ 18	8
C18-CAR 3 $\mu$ M	1659 $\pm$ 360**	4	326 $\pm$ 72*	4
C18-CAR 10 $\mu$ M	772 $\pm$ 82***	3	191 $\pm$ 14**	3
C18-CAR 30 $\mu$ M	638 $\pm$ 98***	4	176 $\pm$ 15***	6

Values obtained when the membrane potential returned to  $-55$  mV after stepping to  $-10$  mV for 5 s. \* $p < 0.05$ , \*\* $p < 0.01$ , \*\*\* $p < 0.001$ .  
doi:10.1371/journal.pone.0041686.t002

CAR and C10-CAR), or long-chain acyl-CARs (e.g. C16-CAR and C18-CAR). Compared to the physiological concentration (3  $\mu$ M), absence of acyl-CAR in the pipette had no impact on  $I_{hERG}$  (data not shown). Raising the concentration of the various acyl-CARs from 3  $\mu$ M to 30  $\mu$ M had no effect on the amplitude of the current (data not shown). Similarly, the kinetics of deactivation of the current were not affected by the various acyl-CARs, whatever their chain length (Table 1). We concluded that CAR and acyl-CAR had no impact on  $I_{hERG}$  when applied intracellularly.

### Long-chain Acylcarnitines Increase $I_{hERG}$ Amplitude and Accelerate Deactivation when Applied Extracellularly

Acyl-CARs of various chain lengths were applied extracellularly. Free CARs (data not shown) or medium-chain acyl-CARs had no impact on the amplitude of  $I_{hERG}$  (fig. 1A). In contrast, 3  $\mu$ M C18-CAR increased the amplitude of the end-pulse current. This effect took about 2 minutes to be complete and occurred at almost

all voltages (fig. 1B). Similar results were obtained with 3  $\mu$ M C16-CAR, another LCAC derivative (data not shown). External application of 3  $\mu$ M C16-CAR for about 4 minutes led to a significant leftward shift of the activation curve without any effect on the availability properties (fig. 2A and 2B). Conversely, C18-CAR did not affect the activation properties while the availability curve was shifted to the right (fig. 2C and 2D). We concluded from these experiments that extracellularly-applied long-chain acyl-CAR increased  $I_{hERG}$  amplitude in a manner, dependent on their chain length.

LCAC also affected deactivation kinetics when they are applied extracellularly, 3  $\mu$ M C16-CAR and C18-CAR significantly increased deactivation kinetic (by about 30–35%), whereas medium-chain acyl-CAR had no effect on deactivation (fig. 3 and Table 1).

### The Effects of Long-chain Acylcarnitines are Dose-dependent

Increasing the concentration of C18-CAR from 1 to 30  $\mu$ M caused an increase in  $I_{hERG}$  amplitude (fig. 4) and deactivation kinetics (Table 2). Similar results were obtained with C16-CAR (data not shown).

### Accelerated Deactivation is not Due to Fatty Acid Alone

In order to understand the specificity of the effect of long-chain acyl-CAR on  $hERG$  channels, we investigated the effects of two long-chain free fatty acids with the same chain length. Extracellular application of 3  $\mu$ M palmitoyl methyl ester (C16:0) or oleyl methyl ester (C18:1) caused a leftward shift of the activation curve with no change in the availability curve, reproducing increase of  $I_{hERG}$  amplitude caused by long-chain acyl-CARs (data not shown). In contrast, long-chain fatty acids did not change the deactivation kinetics (Table 3 and fig. 5). This suggests that the effect of long-chain acyl-CARs on the deactivation of  $I_{hERG}$  was specifically related to long-chain acyl-CAR derivatives.

**Table 3.** Effect of extracellular C16 free fatty acid either alone or in combination with C16-CAR on  $I_{hERG}$  deactivation time constants.

Tau1							
Voltage (mV)	PSS		C16		C16+ C16-CAR		
	Mean $\pm$ SEM	n	Mean $\pm$ SEM	n	Mean $\pm$ SEM	n	
-30	2620.3 $\pm$ 497.6	6	2780.7 $\pm$ 220.7	5	2620.3 $\pm$ 497.6	6	
-20	2661.7 $\pm$ 226.9	6	2131.7 $\pm$ 148.9	5	2661.7 $\pm$ 226.9	6	
-10	2076.7 $\pm$ 85.1	7	2012.8 $\pm$ 122.1	7	2076.7 $\pm$ 85.1	7	
0	2070.5 $\pm$ 133.4	7	1973.2 $\pm$ 135.8	7	2070.5 $\pm$ 133.4	7	
10	2028.8 $\pm$ 116.7	7	1927.7 $\pm$ 113.4	7	2028.8 $\pm$ 116.7	7	
Tau 2							
-30	670.3 $\pm$ 123.6	5	587.5 $\pm$ 52.4	7	370.5 $\pm$ 48.6*	7	
-20	590.1 $\pm$ 87.3	7	522.4 $\pm$ 88.7	7	284.8 $\pm$ 36.2***	7	
-10	381.0 $\pm$ 23.1	7	364.3 $\pm$ 22.5	7	257.0 $\pm$ 29.0***	7	
0	349.3 $\pm$ 24.2	7	337.9 $\pm$ 25.4	7	242.0 $\pm$ 27.3***	7	
10	339.8 $\pm$ 22.6	7	310.8 $\pm$ 13.2	7	236.4 $\pm$ 25.5***	7	

Values obtained when the membrane potential returned to  $-55$  mV after stepping to the voltage indicated in the left column in mV for 5 s. The current was fitted to a two exponential function (see Methods). The values of tau1 and tau2 are expressed in ms. \* $p < 0.05$ , \*\* $p < 0.01$ , \*\*\* $p < 0.001$ .

doi:10.1371/journal.pone.0041686.t003

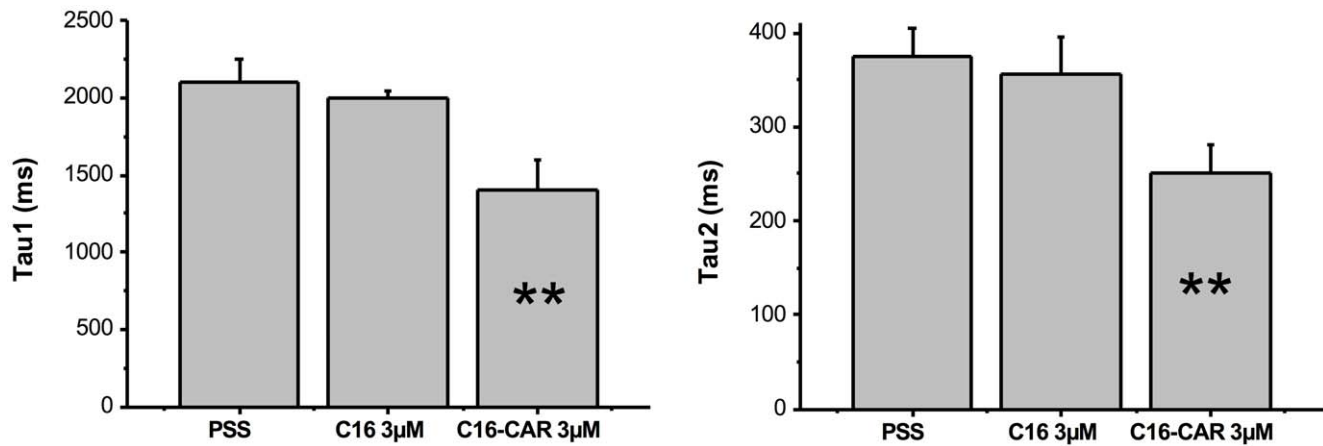


**Figure 5. The effect of extracellular C16 or C16-CAR on deactivation kinetics of  $I_{hERG}$ , when membrane potential returned to  $-55$  mV from a 5sto  $-10$  mV. \*\*  $p < 0.01$ .**  
doi:10.1371/journal.pone.0041686.g005

### Acylcarnitines do not Affect $K_{IR2.1}$ or $Kv7.1/minK$ Channels

To evaluate a possible impact of extracellular acyl-CAR on the  $K_{IR2.1}$  channel, we compared the current in the absence or presence of long-chain acyl-CARs. At concentrations up to  $10 \mu\text{M}$ , C16-CAR has no effect on  $I_{K1}$  amplitude (fig. 6). Application of  $3 \mu\text{M}$  C16-CAR had no effect on  $Kv7.1/minK$  channel amplitude (fig. 7) or kinetics (data not shown).

## Discussion

### Summary of Results

In this study we compare the effects of free carnitine and acyl-CAR on  $hERG$ ,  $Kv7.1/minK$  and  $K_{IR2.1}$  channels. Acyl-CARs with different aliphatic hydrocarbon tail lengths, were applied at different concentrations to both intra- and extracellular sides of the cell membrane. Palmitoyl-carnitine had no effect on  $K_{IR2.1}$  and  $Kv1.7/minK$  at concentrations up to  $10 \mu\text{M}$  but some effects were

observed on the  $hERG$  channel. These effects were specific to extracellular LCAC. Intracellular application of free carnitine or acyl-CARs had no effect on any current, irrespective of the acyl chain length. At the extracellular side of the membrane, free carnitine and medium-chain acyl-CAR up to  $30 \mu\text{M}$  had no effect. Only LCAC had some effects on  $hERG$  current.

When applied extracellularly, LCACs induced increased  $I_{hERG}$  probably due to the leftward shift of the activation for C16-CAR and rightward shift of the availability for C18-CAR. This effect began at  $1 \mu\text{M}$ , a physiological concentration of LCAC, and increased dose-dependently. Since other potassium channels ( $K_{IR2.1}$  and  $Kv7.1/minK$ ) were not sensitive to LCAC, it is likely that these are direct effects on the channel protein and not due to any non-specific effects of the lipophilic compounds on the plasma membrane. These results suggest a tonic regulatory role of physiological concentrations of long-chain acyl-CAR on  $I_{KR}$ .

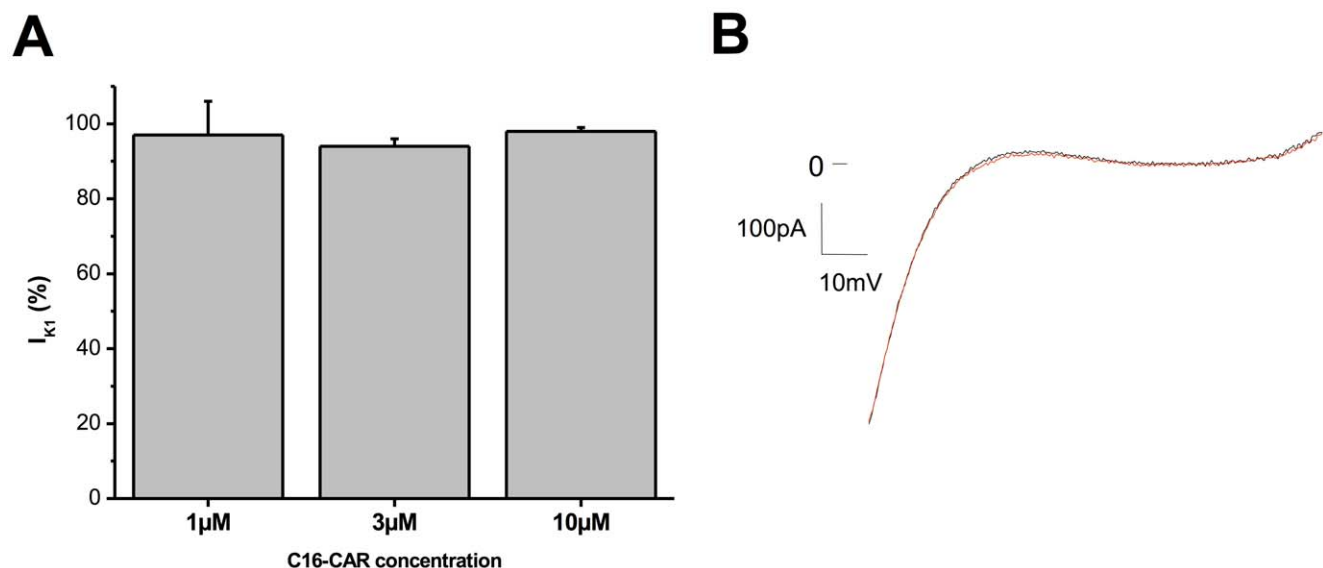


**Figure 6. Effect of C16-CAR on  $I_{K1}$ .** **A**, mean current measured at  $-120$  mV and normalized to the current in PSS ( $n = 7$  cells). **B**, typical example of  $I_{K1}$  elicited by a ramp of voltage between  $-120$  and  $+40$  mV, with (red) or without (black)  $10 \mu\text{M}$  C16-CAR.  
doi:10.1371/journal.pone.0041686.g006

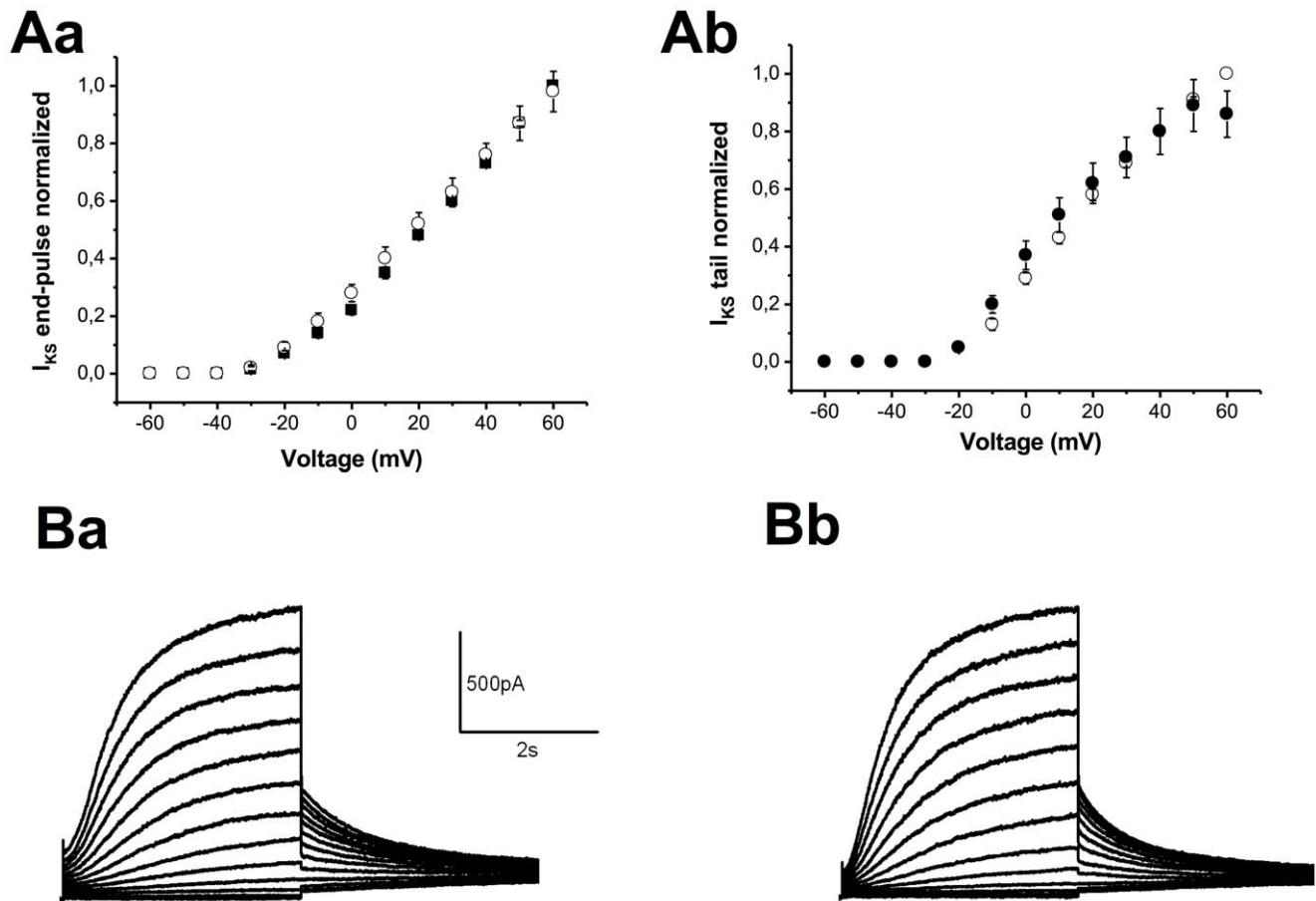


**Figure 7. Effect of 3  $\mu$ M C16-CAR on  $I_{KS}$ .** **A**,  $I_{KS}$ -V curves of the current at the end of the pulse (**Aa**) and peak tail current (**Ab**). **B**, Typical examples of families of currents in the absence (**Ba**) and presence of C16-CAR (**Bb**). doi:10.1371/journal.pone.0041686.g007

### Effects of Long-chain Acylcarnitines on Other Ion Channels

The regulation of ion channels by acyl-CAR has been widely studied in recent years. In every case, the comparison was between high concentrations of LCAC (up to 30  $\mu$ M) and no LCAC, two situations now known to be pathological. Most of these previous studies were focused on the specific effect of C16-CAR. Various effects have been described depending on whether the acyl-CAR was applied extra- or intracellularly and also depending on the technique used to study the currents. Wu and Corr [12] found that C16-CAR applied extra- or intracellularly led to an inhibition of the whole-cell L-type calcium current in guinea-pig ventricular myocytes. Conversely, Liu and Rosenberg [23] found that 1  $\mu$ M C16-CAR increased the open probability of reconstituted cardiac L-type calcium channels in membrane bilayers.  $I_{K,ATP}$  was blocked by micromolar concentrations of C16-CAR when applied to the internal face of the membrane in the inside-out configuration of the patch clamp technique [24]. Sato *et al.* [25] reported that this amphipathic molecule reduced  $I_{K1}$  but only when it is applied at concentrations higher than 10  $\mu$ M. Sato *et al.* reported a reversible blockade of the sodium current associated with a slowing of both activation and inactivation properties when 5  $\mu$ M C16-CAR was applied extracellularly [26]. Rat cardiac ventricular  $I_{TO}$  was inhibited by C16-CAR in a dose-dependent manner when present in the pipette solution, but had no effect

when superfused extracellularly [27]. In agreement with our results, these authors did not observe any effect on  $I_{K1}$  whether the amphipathic molecule was applied intra- or extracellularly at concentrations up to 10  $\mu$ M.

Surprisingly, there has been no previous study of the effects of LCAC on the hERG (or  $I_{KR}$ ) and  $I_{KS}$  even though these channels are considered to be the target of drugs which seek to prevent ventricular fibrillation and sudden cardiac death see [15].

### Effects of Long-chain Acylcarnitines on hERG Channel

From our experiments on HEK293 cells stably expressing hERG, we can infer that LCAC regulate hERG channel activity via an extracellular site. Indeed, long-chain acyl-CARs are associated with an increase in the speed of deactivation of the channel compared to the “pathological” condition where acyl-CAR is absent. This effect is dose-dependent, at least up to 30  $\mu$ M. Both, C16-CAR and C18-CAR increase the amplitude of the current but the mechanism of increased current amplitude is different. C16-CAR induced a shift of the activation curve in the hyperpolarizing direction without any effect on the availability curve. C18-CAR has no effect on the activation curve but provoked a shift in the availability curve in the depolarizing direction. Interestingly, quite similar results were obtained by Wang *et al.* [28] with lysophosphatidylcholine (LPC) having a C16:0 or C18:1 as acyl groups. Changing the positively charged phosphatidylcholine with phosphatidylcholineglycerol was associ-

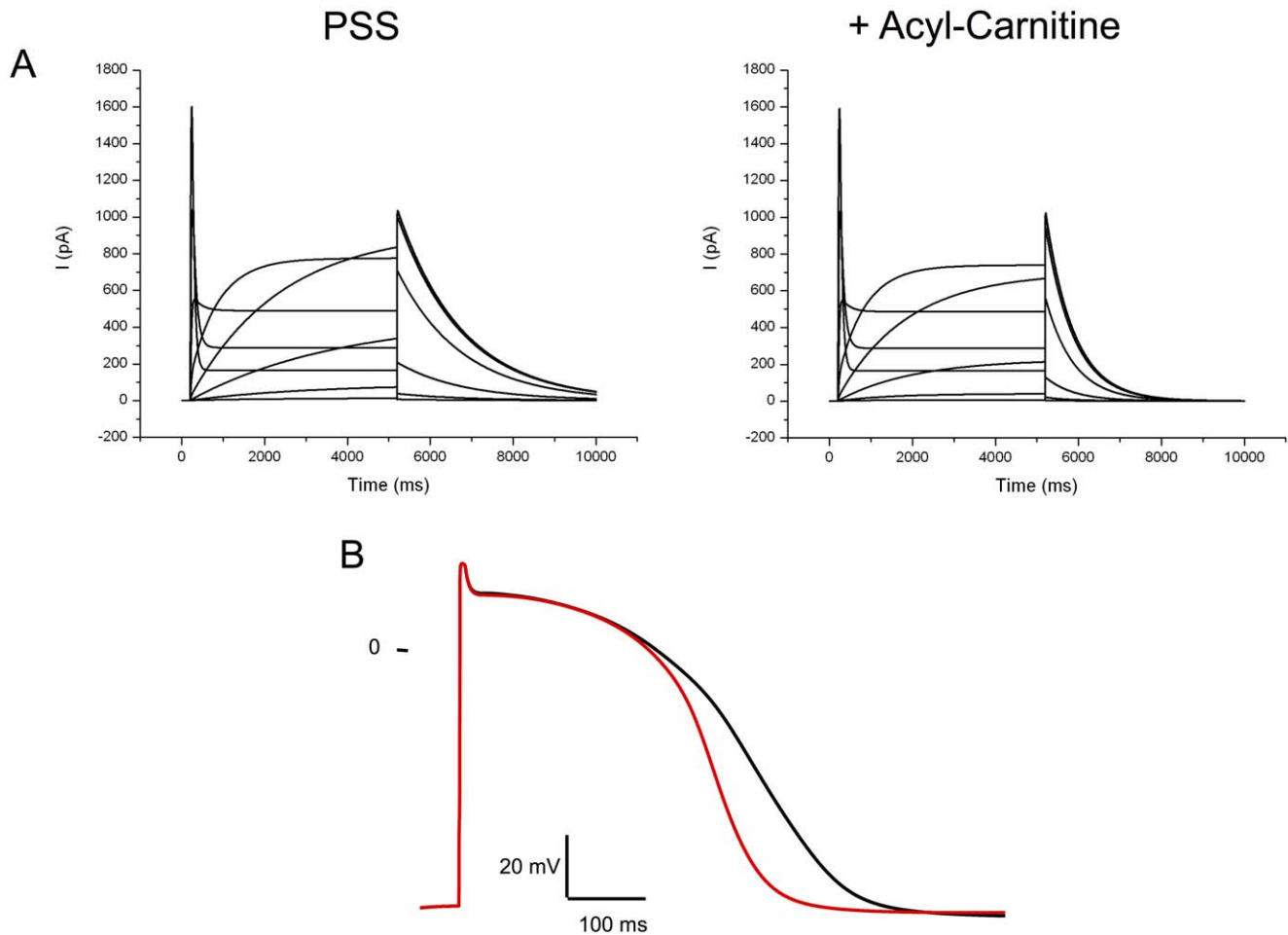


**Figure 8. Computer simulation of the effects of LCAC on  $I_{KR}$  and the human ventricular action potential. A,** families of currents mimicking  $I_{KR}$  with or without acyl-CARs. **B,** action potential profile in the absence of acylcarnitine (black line) or the presence of a physiological concentration of 3  $\mu$ M LCAC (red line). doi:10.1371/journal.pone.0041686.g008

ated with substantial modifications of the effects underlying the important role played by this charged head. These authors concluded that the effects they observed were not due to membrane incorporation of the lipids or to any intracellular signalling pathways currently known to be related to these lipids. They proposed that there must be a direct interaction of the lysophospholipid molecules with the channel protein. However, they also proposed that these lipids could modify hERG activity *via* unidentified pathways. In the present work, we found that acyl-CARs had no effect on the hERG current, at concentrations up to 30  $\mu$ M. So either these lipids do not incorporate into the membrane or their incorporation has no effect on the activity of the ion channel. In contrast, LCAC can incorporate into the plasma membrane and modify membrane fluidity. However, there is no effect of the fatty acids palmitate and stearate that can also integrate the membrane. Also, LCAC does not affect  $K_{IR2.1}$  and  $K_{V7.1}/mink$  currents. Thus, the electrophysiological effects of LCAC on  $I_{hERG}$  are dependent on the aliphatic hydrocarbon tail length but are unlikely to involve changes in plasma membrane properties. These results are in agreement with previously reported cases of cardiac arrhythmias associated with inherited fatty acid oxidation disorders in human. Indeed, Bonnet *et al.* [29] reported that cardiac arrhythmias and sudden death were usually observed in patients with genetic disorders of long-chain fatty acid oxidation

associated with long-chain acyl-CAR accumulation. In contrast, cardiac electrical disturbances were absent in patients with medium-chain fatty acid oxidation deficiency, a condition associated with a specific increase in medium-chain acyl-CAR but normal long-chain derivatives [28].

Our observations suggest that there is a dual interaction of the acyl group and the charged head of the LPC or LCAC with the channel. Since the physiological concentration of LCAC is between 1 and 3  $\mu$ M [5–6], [18], there must be a tonic regulation of hERG channels by long-chain acyl-CAR under physiological conditions.

#### Consequences of Extracellular Accumulation or Depletion of Long-chain Acylcarnitines under Pathological Conditions

Acyl-CAR concentration can reach 10  $\mu$ M in some pathological conditions such as myocardial ischaemia [7], diabetes [8], [9], or genetic fatty acid disorders [10]. Conversely there is a drop in CAR and acyl-CAR cytosolic concentrations in primary systemic carnitine deficiency [2]. All these pathological situations are associated with cardiac arrhythmias and sudden cardiac death [29–32], [2]. Accordingly, hERG regulation by LCAC could play a

role in the cardiac arrhythmias genesis observed in these pathological conditions.

### Consequences for the Action Potential?

An increase of  $I_{KR}$ , the cardiac current encoded by hERG, could lead to a reduction of the action potential duration. However, it is known that this channel inactivates and reactivates very rapidly leading to a higher current during the final repolarisation phase than during the plateau phase of the action potential. Since the deactivation of the current is accelerated, the current during the action potential must be lower. Indeed, Clancy and Rudy [33] reported a case of congenital long QT syndrome due to a mutation of hERG leading to an acceleration of  $I_{KR}$  deactivation kinetics (see also Rudy and Silva [34]). This speeding of deactivation could overcome the effect on the increased amplitude. To investigate this point, we simulated hERG current in the presence and absence of C16-CAR 3  $\mu$ M using Markov equations (see methods). Introducing such a current in the human endocardial ventricular cell model developed by TenTusscher and Panfilov [21] showed that the regulation of the hERG by C16-CAR could be responsible for a pronounced shortening of the

action potential. This indicates that with the absence of carnitine, there must be an increased APD (fig. 8) while the opposite could be induced with an accumulation of LCAC, both conditions being potentially pro-arrhythmic.

### Summary

The results of this study demonstrate that long-chain acyl-CARs have regulatory properties on the hERG channel. These electrophysiological effects were not observed with medium-chain acyl-CARs. This emphasizes the relationship between long-chain fatty acid metabolism and cardiac electrical activity that contribute to cardiac arrhythmias associated with LCAC depletion or accumulation occurring in some pathologies.

### Author Contributions

Conceived and designed the experiments: FF AO TAT PF PB DB FL JYLG. Performed the experiments: FF AO TAT PF PB DB FL JYLG. Analyzed the data: FF AO TAT PF PB DB FL JYLG. Contributed reagents/materials/analysis tools: FF AO TAT PF PB DB FL JYLG. Wrote the paper: FF AO TAT PF PB DB FL JYLG.

### References

- Kodde I, Van der Stok J, Smolenski R, de Jong J (2007) Metabolic and genetic regulation of cardiac substrate preference. *Comp Biochem Physiol A Mol Integr Physiol* 146(1): 26–39.
- Stanley C (2004) Carnitine deficiency disorders in children. *Ann N Y Acad Sci* 1033: 42–51.
- Ferrari R, Merli E, Cicchitelli G, Mele D, Fucili A, et al (2004) Therapeutic effects of L carnitine and propionyl-L-carnitine on cardiovascular diseases: a review. *Ann N Y Acad Sci* 1033: 79–91.
- McGarry J, Mills S, Long C, Foster D (1983) Observations on the affinity for carnitine, and malonyl-CoA sensitivity, of carnitine palmitoyltransferase I in animal and human tissues. Demonstration of the presence of malonyl-CoA in non-hepatic tissues of the rat. *Biochem J* 241: 21–28.
- Opalka J, Gellerich F-N, Zierz S (2001) Age and sex dependency of carnitine concentration in human serum and skeletal muscle. *Clin Chem* 47: 2150–2153.
- Jones M, Goodwin S, Amjad S, Chalmers R (2005) Plasma and urinary carnitine and acylcarnitines in chronic fatigue syndrome. *Clin Chim Acta* 360: 173–177.
- Ford D, Han X, Horner C, Gross R (1996) Accumulation of unsaturated acylcarnitine molecular species during acute myocardial ischaemia: metabolic compartmentalization of products of fatty acyl chain elongation in the acylcarnitine pool. *Biochemistry* 35(24): 7903–7909.
- Lopaschuk G (1996) Abnormal mechanical function in diabetes: relationship to altered myocardial carbohydrate/lipid metabolism. *Coron Artery Dis* 7(2): 116–123.
- An D & Rodrigues B (2006) Role of changes in cardiac metabolism in development of diabetic cardiomyopathy. *Am J Physiol Heart Circ Physiol* 291(4): H1489–H1506.
- Longo N, Amat di San Filippo C, Pasquali M (2006) Disorders of carnitine transport and the carnitine cycle. *Am J Med Genet C Semin. Med Genet* 142C(2): 77–85.
- DaTorre S, Creer M, Pogwizd S, Corr P (1991) Amphipathic lipid metabolites and their relation to arrhythmogenesis in the ischemic heart. *J Mol Cell Cardiol* 23 Suppl 1: 11–22.
- Wu J, Corr P (1992) Influence of long-chain acylcarnitines on voltage-dependent calcium current in adult ventricular myocytes. *Am J Physiol* 263: 410–417.
- Wu J, Corr P (1995) Palmitoylcarnitine increases  $[Na^+]_i$  and initiates transient inward current in adult ventricular myocytes. *Am J Physiol* 268: H2405–H2417.
- Brugada R, Hong K, Cordeiro J, Dumaine R (2005) Short QT syndrome. *CMAJ* 173: 1349–1354.
- Champéroux P, Viaud K, El Amrani A, Fowler J, Martel E, Le Guennec J-Y, Richard S (2005) Prediction of the risk of Torsade de Pointes using the model of isolated canine Purkinje fibres. *Br J Pharmacol* 144: 376–385.
- Schimpf R, Wolpert C, Gaita F, Giustetto C, Borggrefe M. (2005) Short QT syndrome. *Cardiovasc Res* 67: 357–366.
- Hedley P, Jorgensen P, Schlamowitz S, Wangari R, Moolman-Smook J, et al. (2009) The genetic basis of long QT and short QT syndromes: a mutation update. *Human Mutat* 30(9): 1256–1266.
- Su X, Han X, Mancuso D, Abendschein D, Gross R (2005) Accumulation of long-chain acylcarnitine and 3-hydroxy acylcarnitine molecular species in diabetic myocardium: identification of alterations in mitochondrial fatty acid processing in diabetic myocardium by shotgun lipidomics. *Biochemistry* 44: 5234–5245.
- Zhou Z, Gong Q, Ye B, Fan Z, Makielski JC, et al. (1998). Properties of HERG channels stably expressed in HEK 293 cells studied at physiological temperature. *J Biophys* 74: 230–41.
- Pascarel C, Hongo K, Cazorla O, White E, Le Guennec J-Y (1998) Different effects of gadolinium on  $I_{KR}$ ,  $I_{KS}$  and  $I_{K1}$  in guinea-pig ventricular myocytes. *Br J Pharmacol* 124: 356–360.
- Ten Tusscher K & Panfilov K (2006) Alternans and spiral breakup in a human ventricular model. *Am J Physiol Heart Circ Physiol* 291: H1088–H1100.
- Fink M, Noble D, Virag L, Varro A, Giles W (2008) Contributions of HERG K<sup>+</sup> current to repolarization of the human ventricular action potential. *Prog Biophys Mol Biol* 96(1–3): 357–376.
- Liu Q-Y, Rosenberg R (1996) Activation and inhibition of reconstituted cardiac L-type calcium channels by palmitoyl-L-carnitine. *Biochem Biophys Res Comm* 228: 252–258.
- Haruna T, Horie M, Takano M, Kono Y, Yoshida H, et al. (2000) Alteration of the membrane lipid environment by L-palmitoylcarnitine modulates KATP channels in guinea-pig ventricular myocytes. *Pflügers Arch* 441: 200–207.
- Sato T, Arita M, Kiyosue T (1993) Differential mechanism of block of palmitoyl lysophosphatidylcholine and of palmitoylcarnitine on inward rectifier K<sup>+</sup> channels of guinea-pig ventricular myocytes. *Cardiovasc Drugs Ther* 7: 575–584.
- Sato T, Kiyosue T, Arita M (1992) Inhibitory effects of palmitoylcarnitine and lysophosphatidylcholine on the sodium current of cardiac ventricular cells. *Pflügers Arch* 420: 94–100.
- Xu Z, Rozanski G (1998) K<sup>+</sup> current inhibition by amphiphilic fatty acid metabolites in rat ventricular myocytes. *Am J Physiol Cell Physiol* 275: C1660–C1667.
- Wang J, Zhang Y, Wang H, Han H, Nattel S, et al. (2004) Potential mechanisms for the enhancement of HERG K<sup>+</sup> channel function by phospholipids metabolites. *Br J Pharm* 141: 586–599.
- Bonnet D, Martin D, De Lonlay P, Villain E, Jouvet P, et al. (1999) Arrhythmias and conduction defects as presenting symptoms of fatty acid oxidation disorders in children. *Circulation* 100: 2248–2253.
- Bergner D & Goldberger J (2010) Diabetes mellitus and sudden cardiac death: what are the data? *Cardiol J* 17(2): 117–129.
- Pappone C & Santinelli V (2010) Cardiac electrophysiology in diabetes. *Minerva Cardio angi* 58(2): 269–276.
- Siscovick D, Sotoodehnia N, Rea T, Raghunathan T, Jouven X, et al. (2010) Type 2 diabetes mellitus and the risk of sudden cardiac arrest in the community. *Rev Endocr Metab Disord* 11(1): 53–59.
- Clancy C & Rudy Y (2001) Cellular consequences of hERG mutations in the long QT syndrome: precursors to sudden cardiac death. *Cardiovasc Res* 50(2): 301–313.
- Rudy Y, Silva J (2006) Computational biology in the study of cardiac ion channels and cell electrophysiology. *Q Rev Biophys* 39: 57–116.